ICES Journal of Marine Science, 2024, Vol. 81, Issue 1, 145–161
https://doi.org/10.1093/icesjms/fsad186
Received: 15 December 2022; **revised:** 1 November 2023; **accepted:** 2 November 2023
Advance access publication date: 6 December 2023
Original Article

Simultaneous Bayesian estimation of size-specific catchability and size spectrum parameters from trawl data

Kyle J. Krumsick* **and Eric J. Pedersen**

Department of Biology, Concordia University, 7141 Sherbrooke W., Montreal, QC H4B 1R6, Canada
*Corresponding author. Department of Biology, Concordia University, 7141 Sherbrooke W., Montreal, QC H4B 1R6, Canada.
E-mal: Kyle.Krumsick@dfo-mpo.gc.ca

Abstract

Fisheries-independent surveys are a critical tool for monitoring marine populations and communities. However, considerations must be made to account for variable-size-based catchability. The size-specific catchability function is therefore key for estimating size distributions, but often requires extensive data sets or specialized field experiments to determine. We develop a Bayesian model capable of simultaneously estimating both a size-based catchability curve and species-specific size spectrum parameters from trawl data by assuming that individual species size spectra follow a theoretically derived parametric size spectrum model. The resulting model provides a means of estimating catchability and size spectra within an adaptive framework capable of accommodating confounding factors such as vessel power and fish density, potentially allowing for improved biomass and productivity estimates. We demonstrate the application of this model using 15 years of Greenland Halibut (*Reinhardtius hippoglossoides*) survey data from Nunavut to determine size-specific catchabilities and assess whether the size spectrum of Greenland Halibut has changed across the time series. While size spectrum parameters for this stock were not found to vary, we did find evidence of time-varying catchability parameters across the study period.

Keywords: single species size spectrum; Bayesian modeling; size spectra; Greenland Halibut; Nunavut; size selectivity

Introduction

Effective ecosystem-based management of marine populations and communities requires monitoring tools capable of detecting effects of multiple interacting drivers, both ecological and anthropogenic (Tam et al. 2017). The size spectrum of an assemblage is the relationship between the abundance of organisms to their body size, such that smaller, lower-trophic-level organisms will be more abundant than larger ones (Sheldon and Parsons 1967, Rice and Gislason 1996). Size spectra analyses have been used to inform scientists and managers about variation in top-down and bottom-up drivers of marine communities (Rice and Gislason 1996, Shin et al. 2005, Blanchard et al. 2009). Measuring size distributions in marine ecosystems can be challenging, however, as we cannot directly observe fish in their natural habitat without specialized equipment, removing potential estimation techniques applicable to terrestrial or shallow-water resources, such as visual surveys (e.g. Turner and Mackay 1985, Thompson and Harwood 1990, Margalida et al. 2011). One of the most common tools to make inferences about the relative size distribution of marine species is to use empirical size distributions from trawl surveys (Pennington 1985, Smith 1990, Chen et al. 2004).

In principle, a trawl sweeping a given area of sea floor should provide an accurate estimate of the density (biomass per unit area) of different species or size classes of fish in the area, which can be used in turn to estimate the size spectrum for the area (e.g. Daan et al. 2005, Edwards et al. 2017). However, trawls will never capture all the fish present in the swept area. Fish may slip through the net if they are below optimal size (Engås and Godø 1989, Gabr et al. 2007), detect the trawl approaching and swim out of the path (Albert et al. 2003, 2006, Robert et al. 2020), pass above the opening of the trawl (Jørgensen 1997, Dremière et al. 1999), or pass underneath the trawl (Engås and Godø 1989, Ingólfsson and Jørgensen 2006, Ryer 2008). The average fraction of the available individuals in an area captured by a given trawl under local environmental conditions is referred to as the catchability of the trawl, and it varies according to the fishing gear used, the morphology and behavior of a given fish species, and the abiotic and biotic conditions at the fished site (Arreguín-Sánchez 1996).

Catchability varies not only with environmental conditions and among species, but also with body size within a given species: smaller fish can slip through nets more easily (Millar 1992, Peng et al. 2013, Stepputtis et al. 2016) and larger fish may be able to swim away from the net more effectively, or spend more time away from the bottom (Benoít and Swain 2003, Winger et al. 2010, Smith and Taylor 2014). The relative catchability of different size classes of fish by a given survey is referred to as the size selectivity curve method (Millar and Fryer 1999). Relative catchability can vary depending on a range of gear- and survey-specific (Sissenwine and Bowman 1978, Engås and Godø 1986, Harley et al. 2001, Jones et al. 2008), species-specific (Godø et al. 1999, Benoît and Swain 2003, Brodziak et al. 2004, Barange et al. 2005), and environment-specific conditions (Macpherson and Gordoa 1992, Gordoa et al. 2000, Thorson et al. 2012).

If the size-specific catchability curve is not accounted for when estimating the shape of a size spectrum, it will bias estimates of relative abundances of different size classes, either under- or over-estimating the relative abundance of larger individuals compared to smaller individuals, depending on the shape of the catchability curve. For instance, if small fish are

able to pass through the mesh of the trawl whereas larger fish cannot, the relative abundance of small fish will be on average lower in the trawl than what was present in the area swept by the trawl.

To account for reduced catchability of small fish, past size-spectrum studies have typically only used size frequency data for size classes larger than the peak size class in observed data (i.e. the descending slope of the observed size-abundance relationship) when estimating the slope of size spectra (e.g. Rice and Gislason 1996, Daan et al. 2005, Krumsick and Fisher 2020). However, this assumption does not account for the possibility of catchability decreasing with size for larger fish (e.g. due to gear avoidance or location in the water column). If this scenario occurs, the number of large individuals caught by a trawl will be less than what was in the path of the trawl. As a result, the shape of the size spectrum to the right of the empirical peak will underestimate the relative fraction of larger size classes. If the true shape of the size-specific catchability curve were known, both forms of bias could be accounted for by scaling observed catches by the inverse of the catchability curve prior to estimating the spectrum.

Size-specific catchability curves have been estimated for a few gear types (e.g. Cadigan et al. 2006), generally based on comparing catch-at-size for a given gear with catch-at-size to a gear with a smaller mesh size or specialized cod ends to prevent escape (Millar and Fryer 1999). However, size-selectivity of a given species can depend on a wide range of local factors. Given the wide breadth of factors influencing the catchability of a species, using published size-specific catchability curves estimated in different environmental conditions introduces several assumptions regarding the applicability of the published findings to novel situations. Furthermore, many gear types do not have comparable published estimates apart from their target species (Rosing and Wieland 2015, Larsen et al. 2018). Species of limited economic value are often simply ignored, which can complicate multispecies ecosystem analyses.

The issue of confounding factors influencing the catchability of a given species resulting in potentially inaccurate size spectrum slope estimates could be avoided if both the shape of the size-frequency distribution and the size-specific catchability curve could be estimated for individual species from trawl data alone. This is not possible for arbitrarily shaped size-frequency and catchability curves, as it would be impossible to determine if low catches of a given size bin were due to low frequency or low catchability for that size bin. However, we do not expect either the size-frequency or catchability curves to take on arbitrary shapes. The functional form of the species-specific size–frequency curve can be predicted based on metabolic theory and species-specific parameters (Andersen and Beyer 2006), and the expected functional form of the species-specific catchability curve can be predicted based on the gear (type, mesh size, and mesh geometry) and behavior of the target species. If it is possible to sufficiently constrain the possible shapes of the two curves based on prior information, it may be possible to estimate both curves from trawl data alone.

The purpose of this study is 2-fold. First, we demonstrate and evaluate a novel statistical model that allows the simultaneous estimation of both a single-species size spectrum function and a size-specific catchability function from a single set of trawl data. This model structure is flexible enough to allow for temporally and spatially varying parameters, to allow for changing environmental and survey conditions. Second, we demonstrate how to estimate the parameters for this model in a Bayesian framework using the Hamiltonian Monte Carlo algorithm implemented in the Stan software package (Stan Development Team 2022) using fisheries-independent survey data for Greenland Halibut (*Reinhardtius hippoglossoides*) from the Nunavut region. We use a series of nested models to determine if there is evidence of changing size-spectrum or size-specific catchability parameters in this stock across the study period.

Changing single-species size spectrum parameters indicate various phenomenon, depending on the nature of the parameter changes, such as variation in the amount energy available to the individuals (thus influencing their potential for growth), changing energy requirements for the species (Law et al. 2009, Mary and Poggiale 2013, Chongliang et al. 2016), variation in background mortality (Chongliang et al. 2016), spatial shifts in species distributions (Lefort et al. 2015, Xu et al. 2021), changing ocean conditions and other sources of environmental variability (Yvon-Durocher et al. 2011, Woodworth-Jefcoats et al. 2013, Zhang et al. 2015), and potentially of greatest concern to modern fisheries, whether fishing mortality has significantly influenced the size structure of a given species as a whole (e.g. Andersen and Pedersen 2009, Rochet and Benoît 2011, Jacobsen et al. 2013, Marin et al. 2023).

Greenland Halibut is one of the most commercially important fisheries in Nunavut (Government of Nunavut 2016), with the fishery steadily expanding since the late 1990s, such that 15 935 t were caught in 2019, a 336% increase from catches in 1999, with a value of ∼$101 million landed value (Treble and Nogueira 2020). This value represents 60–90% of the total landed harvest of the Nunavut offshore fisheries. With the expansion of any fishery, questions regarding sustainability often arise. Although no significant changes have been reported in the overall biomass, abundance, or recruitment indices, potential changes to the single species size spectrum could still result from fishing activities (Law and Grey 1989, Heino et al. 2015).

Methods

Survey data

Annual fall surveys of the Nunavut shelf, encompassed by NAFO subdivision 0 (NAFO 2020), have been conducted between 1999 and 2019 (Fig. 1). Despite the 20-year range, only 15 years were modeled as several years did not have relevant survey data or covered more inshore areas with questionable comparability to the other years. Individual fishing trawls, or sets, were conducted at randomly selected locations with depths ranging from 401 to 1500 m, using an Alfredo III bottom trawl with 20 mm codend mesh. The target tow duration was 30 min at a towing speed of three knots, with sets being conducted throughout the 24-h period. A primary species of focus on this survey is the Greenland Halibut, or Turbot, due to its recent increase in economic importance. As such, total lengths, the length of a fish measured from the tip of the snout to the tip of the tail, and, frequently, the whole weight of caught Greenland Halibut were obtained during the survey. In cases where large quantities were caught, a random subset of the total sample was taken. No correction was done for subsampling nor was the subsample size distribution ex-

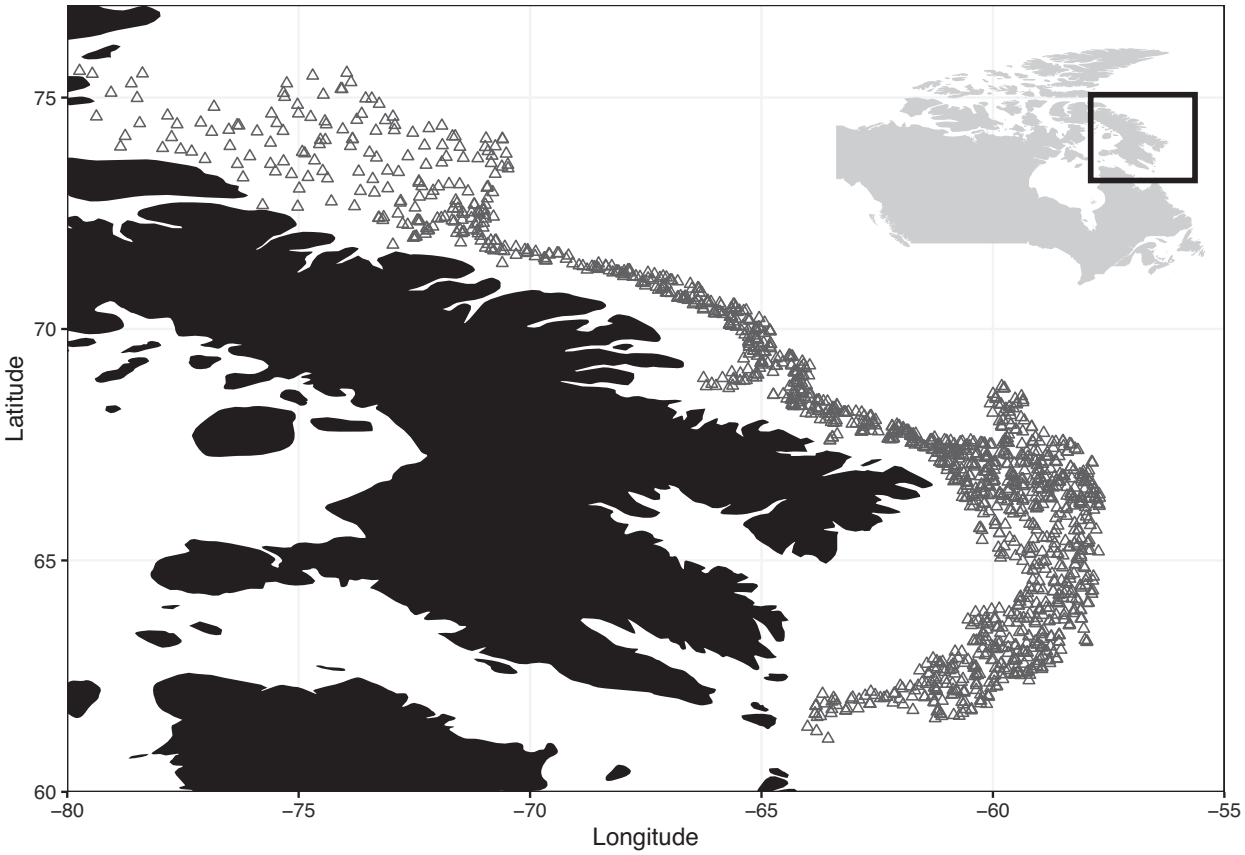

Figure 1. Map of study area along the Nunavut shelf. Triangles represent the trawl locations to which our model was fit to Greenland Halibut trawl data between 1999 and 2019.

panded to the total catch, and the selection was assumed to be a representative random sample.

The data from the annual fall survey conducted by Fisheries and Ocean Canada does have the limitation that it does have the same spatial coverage between years. To ensure that the years remained comparable, a couple of years of data were removed from the analysis. In one situation, the year 2009, the number of sets was too low to conduct an analysis with a total of 184 individual fish measured. Years were also removed if they sampled a vastly different location, such as in 2007, when the survey was conducted inshore and observed an elevated number of juvenile fish relative to the other years. The remaining sets were kept as they were situated along the shelf and consisted of similar depth ranges.

The model

Our prediction for the shape of the observed size distribution of individuals across trawls was theoretically determined by two key processes: a species-specific size spectrum and a peak-logistic size-specific catchability curve (Fig. 2). The first of these processes is the relationship that relates the size of the species to the expected abundance (count per unit area) within the ecosystem. We would expect to see more smaller individuals than large ones considering natural mortality as well as from a bioenergetic perspective. The second process, the peak-logistic size-specific catchability curve, reflects the probability that a fish of a given size in the path of the trawl will be caught. Small fish are anticipated to pass through the net until they reach an optimal size, while large fish will have a higher swimming endurance and are more capable of evading a trawl.

The first process influencing the size distribution of a species is the species-specific size spectrum. Andersen and Beyer (2006) derived an equation for the expected equilibrium size-spectrum for a single consumer species under the assumptions of conservation of mass, a power-law distribution of the community size spectrum, linear functional responses, power-law scaling of metabolic rates with size, a log-normal size-selection feeding function, and constant mass-specific reproduction rates.

The equilibrium size spectrum for a given species [Equation 11 in Andersen and Beye (2006), modified to aid in model convergence] is:

$$N(m) = \left\{ km^{\Delta r - r - s}\left[1 - \left(\frac{m}{m_\infty}\right)^{\Delta r}\right]^{[S/\Delta r]-1} \quad if\ m \geq m_{min} \right\}, \quad (1)$$
$$\left\{ 0 \quad if\ m < m_{min} \right\}$$

where N(m) is the concentration of individuals present in the population at a given location of body size m (here measured as the mass of the individual). Concentration is measured in units of *individuals/kg/km*^{2}, so the density of individuals per km^2 between body sizes m_1 and m_2 at the given location would be $\int_{m_1}^{m_2} N(m)dm$. The parameter m_∞ is the maximum mass for the given species (assumed to be the size where the rate of energy assimilation equals the rate of energy loss due to maintenance), r is a parameter relating maintenance energy

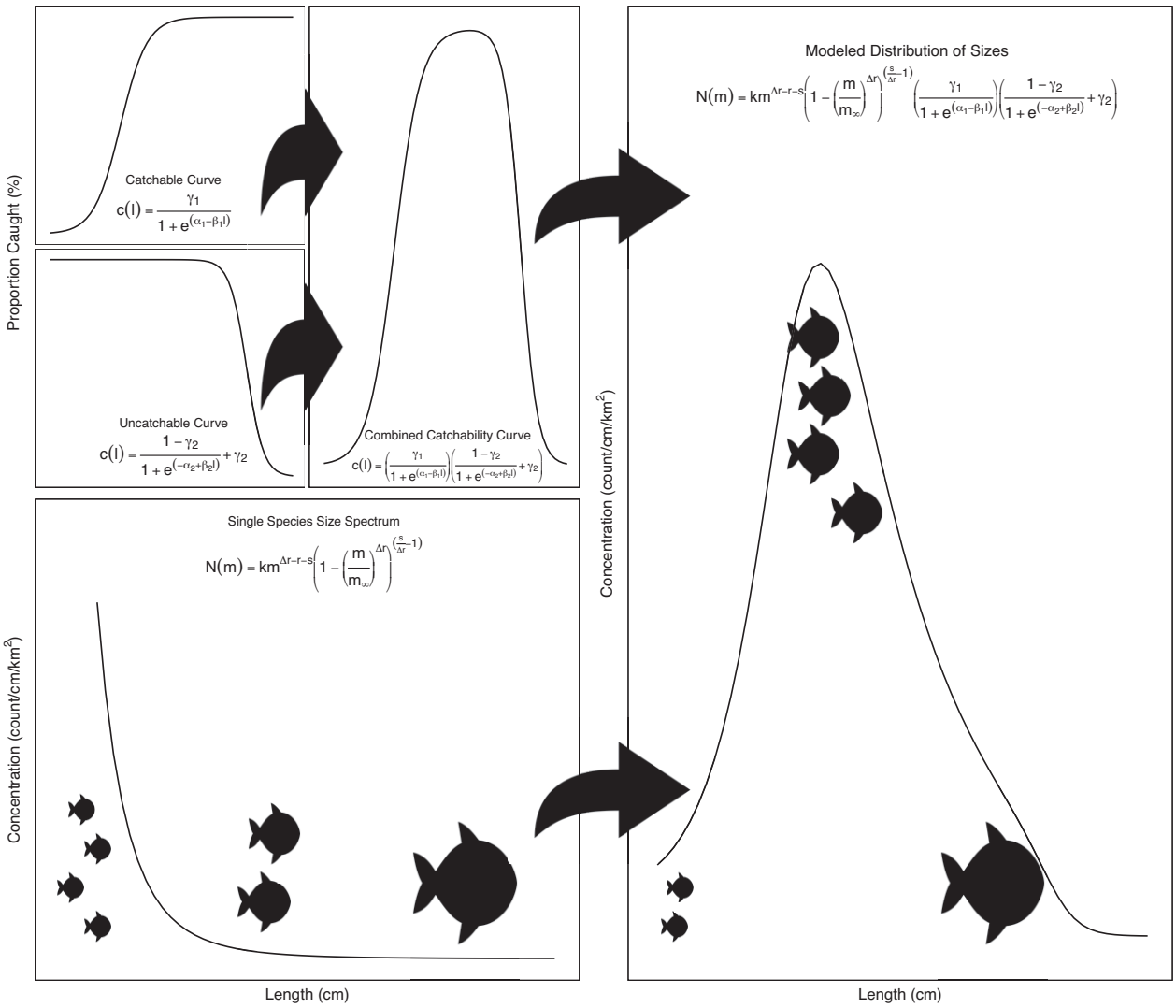

Figure 2. Conceptual diagram outlining the flow of logic for the construction of the model for predicting the observed distribution of sizes. A catchable curve, representing the ability of small fish to pass through a trawl, and an uncatchable curve, representing the ability of large fish to outswim or otherwise evade a trawl, are combined together to create a dome-shaped catchability curve. When combined together with the single-species size spectrum, an indication of fish abundance theoretically in the path of the trawl, we obtain our predicted distribution of abundance at size within the trawl.

costs to body size, s is the ratio of the natural mortality rate to food assimilation rate, and Δr is the difference between the exponent for how maintenance scales with body size and the exponent for how food intake scales with body size (parameter n in Andersen and Beyer 2006). The parameter k is a scaling coefficient, defined so that the definite integral of $N(\mathrm{m})$ from m_{min} (the minimum size of the fish) to m_∞ equals the total biomass or biomass density of the species in the sampled area. Equation (1) will demonstrate an approximately log-linear descending slope until it approaches the maximum size of the fish. As m approaches m_∞, $N(\mathrm{m})$ will decline asymptotically to 0, implying that the slope of the single-species size spectrum will become increasingly negative as m approaches m_∞.

Equation (1) gives the concentration of fish by mass; however, trawl surveys typically measure fish abundance by length. Equation (1) can be converted into a function of length if fish mass scales allometrically with body length as $m \sim g(l) = al^b$, by using the method of transformation of distributions via monotone functions (i.e. $N(l) = |\frac{dg(l)}{dl}| \cdot N(g(l))$; Wood 2005). This gives:

$$N(l) = \begin{Bmatrix} abl^{b-1}.N\left(al\right)^b & if\ l \geq l_{min} \\ 0 & if\ l < l_{min} \end{Bmatrix}. \quad (2)$$

We used log-linear regression to estimate the parameter values of the length–weight relationship for Greenland Halibut in Nunavut as $a = 0.004$ (538 g) and $b = 3.158$ using the subset of the trawl data where both lengths and weights were measured for individual fish.

The function $N(\mathrm{l})$ predicts the concentration of fish at any given length, with units of individuals $\cdot$ cm^{-1} $\cdot$ km^{-2}. This function can be translated into predictions about counts of fish in specific size bins by taking the integral of the function between the lower and upper ends of the size bin [i.e. $\int_{l_0}^{l_1} N(l)dl$]. As our data was collected in equal-width length bins, we approximated this integral using the midpoint rule; i.e. $\int_{l_c+\frac{w}{2}}^{l_c+\frac{w}{2}} N(l)dl \approx N(l_c) \cdot w$, where l_c is the length at the mid-

point of each bin, and w the width of each in cm. For constant-width bins, this is just Equation (2) multiplied by w, which can be absorbed into the scaling coefficient k in Equation (1). The resulting integral has units of *individuals*. This approximation should be reasonable as long as the bin width is small relative to the difference between maximum and minimum size of the fish. To test this assumption, we compared the ratio of the approximate integral to the numerical evaluation of the definite integral of Equation (1) (calculated by adaptive quadrature using the "integrate" function in R), across the range of 1 cm length bins observed in the data (15–101 cm) using posterior mean parameter estimates from the time-variant Bayesian model fit below. We found that the midpoint approximation to the integral was within 0.1% of the true definite integral for all size classes.

The second process assumed to be affecting the shape of the observed size distribution was the size-specific catchability or selectivity curve (i.e. the average proportion of fish at a given length present in the trawled location that would be caught by the trawl). Since larger fish are more likely to stay trapped in a net, but that ability to swim away from an approaching net also likely increases with size (Smith and Taylor 2014), we assumed that catchability was the product of a logistic function and a shifted logistic function:

$$c(l) = \frac{\gamma_1}{1 + e^{(\alpha_1 - \beta_1 l)}} \cdot \left[\frac{(1 - \gamma_2)}{1 + e^{(-\alpha_2 + \beta_2 l)}} + \gamma_2 \right], \tag{3}$$

where the parameters β_1 and β_2 are both greater than or equal to 0. Equation (3) describes a unitless length-specific catchability curve. The value of $c(l)$ indicates the probability of a fish of length l being caught by a given survey when it is present in the region swept by the survey gear. The parameter, γ_1, is the maximum catchability of the survey, ranging between 0 and 1. For gear that was designed to perfectly catch all the target sizes in the trawl, the absolute catchability would be 1. However, more often than not, there is a certain amount of escapement from the size classes of highest catchability and therefore this value is often <1. From trawl data alone, we cannot determine what proportion of the population present in the trawl path was actually caught for the optimal size classes. However, we can determine the relative catchability of the various size classes to the size class of highest catchability, which could be multiplied by a γ_1 if the proportion of the size class with highest catchability was later determined through alternative methods to produce the absolute catchabilities for each size class. Therefore, as we can only truly measure relative catchability from trawl data alone, we set $\gamma_1 = 1$ to represent maximum catchability (this parameter would be discussed in further detail later). The parameters α_1 and β_1 affect, respectively, the minimum catchability and rate of increase with length of the ascending logistic curve. The minimum catchability (i.e. at length 1 = 0 cm) would be $\frac{\gamma_1}{e^{\alpha_1}}$, the midpoint of the ascending logistic curve will occur at α_1/β_1, and the derivative of the curve at the midpoint will be $\gamma_1\beta_1/4$. The second half of the equation describes a descending logistic curve, representing the fish's ability to avoid fishing gear with larger sizes due to greater swimming efficiency. This curve is the left-hand descending size-specific catchability curve and represents processes that make a population uncatchable. Therefore, for simplicity, this curve will be referred to as the uncatchable curve as per Smith and Taylor (2014). The minimum fraction of γ_1 that remains catchable even at the largest fish sizes is described by the parameter γ_2. The parameters α_2 and β_2 affect maximum catchability at 0 length and the slope of the portion of the catchability curve with size.

The curve described by Equation (3) can take on a variety of shapes, depending on the value of the parameters. If $\beta_1 > 0$ but $\beta_2 = 0$o, the curve will follow a traditional S-shaped logistic catchability curve, demonstrating an increase in catchability as a species increases in size. If $\beta_1 = 0$ but $\beta_2 > 0$, catchability will decline with length, with a minimum catchability of γ_2 as length goes to infinity. If both β_1 and β_2 are positive, the curve will be an asymmetric dome-shaped curve, with the width of the plateau of the dome and the magnitude of the asymmetry determined by the α and β parameters of the two curves.

Assuming that the species-specific size spectrum [Equation (2)] accurately reflects the concentration of individuals of a given length in the target population, and the catchability curve [Equation (3)] accurately models the proportion of that population at each length that are caught by the net, the average number of individuals in a given size bin with a midpoint l captured in the survey trawl is given by:

$$T(l)_{obs} = N(l) \cdot c(l). \tag{4}$$

Equation (4) assumes that the average number of individuals in a given size bin $l_{l-w/2} : l_{l+w/2}$ is proportional to the concentration of individuals at the midpoint of the bin given by Equation (2) times the size-selectivity at the midpoint of the bin given by Equation (3). As with Equation (2), we are assuming that catchability does not vary rapidly in any given length bin, so it is reasonable to use the catchability at the midpoint of each bin to represent the average catchability across the bin.

Estimating model parameters with trawl data

The model was coded into Stan language using the rstan package in R (R Core Team 2022, Stan Development Team 2022). See Appendix 1 available in Supplementary materialfor Stan model code. The single-species size spectrum equation assumes a minimum possible size of individual >0 cm, as otherwise the size spectrum would not have a finite integral, as length concentration would approach infinity as length approached 0 cm. Therefore, for the purposes of fitting our model, we set the minimum possible size of fish to be 15 cm, reflecting a size category smaller than the smallest observed Greenland Halibut. We modeled the number of individuals caught per bin as a negative binomially distributed random variable using the mean/overdispersion parameterization of the negative binomial (White and Bennetts 1996, NegBinomial2 in Stan):

$$n_1 \sim Negbin\left[\mu(l), \phi\right]. \tag{5}$$

Where the mean count in a given size bin $\mu(l)$ is given by Equation (4), and the parameter ϕ is an inverse overdispersion parameter, where higher values of ϕ correspond to lower levels of overdispersion: $Var[n_l] = \mu(l) + \frac{\mu(l)^2}{\phi}$ (Stan Development Team 2022).

Using a negative binomial distribution for counts allowed for over-dispersion in counts compared with either a multinomial distribution or a Poisson model for counts. Overdispersed counts are an expected feature of this kind of data, as many marine species show patterns of size-specific aggregation and temporally size-specific patterns such as recruitment pulses.

Table 1. Parameter definitions, constraints, and priors for the presented hierarchical model.

Parameter	Definition	Units	Priors for global parameter means	Priors for random effect standard deviation	Constraints	Reference for prior
Δr	Difference between maintenance and food intake	None	Normal	Half-normal	Lower = 0	West et al. (2001), Andersen and Beyer (2006)
			$\mu = 0.25$ $\sigma = 0.15$	$\sigma = 0.125$	Upper = 1.25	
r	Maintenance	None	Normal	Half-normal	Lower = 0	West et al. (2001), Andersen and Beyer (2006)
			$\mu = 1$ $\sigma = 0.25$	$\sigma = 0.5$	Upper = 1.5	
s	Ratio of mortality rate to food assimilation rate	None	Normal	Half-normal	Lower = 0	Andersen and Beyer (2006)
			$\mu = 0.84$ $\sigma = 0.25$	$\sigma = 0.25$	Upper = 1	
$\mathbf{m}_\infty$	Maximum size	g	Exponential	Normal	Lower = maximum measured size	Coad and Reist (2018)
			$\beta = 0.00\,025$	$\sigma = 22\,500$	Upper = 45 000	
γ_2	Proportion of the maximum catchability that becomes uncatchable at large sizes	None	Uniform	Uniform	Lower = 0	None
					Upper = 1	
α_1	Ascending catchability curve midpoint parameter	None	Normal	Half-normal	Lower = 0	Harley et al. (2001)
			$\mu = 3.47$ $\sigma = 3$	$\sigma = 3$	Upper = 100	
β_1	Ascending catchability curve steepness parameter	1/cm	Normal	Half-normal	Lower = 0	Harley et al. (2001)
			$\mu = 0.09$ $\sigma = 0.06$	$\sigma = 0.06$	Upper = 1	
α_2	Midpoint parameter of logistic curve for size-specific decreases in catchability	None	Uniform	Uniform	Lower = 0	None
					Upper = 110	
β_2	Steepness parameter of logistic curve for size-specific decreases in catchability	1/cm	Uniform	Uniform	Lower = 0	None
					Upper = 1	

Because we implemented a hierarchical model such that an overall mean and standard deviation were estimated for the combined data with individual years allowed to vary from this mean. Priors for this mean value, where possible, including the published mean and standard deviation were obtained from the literature. The prior standard deviation, used in the estimation of the variance of each year around the global mean, was kept at a minimum of the standard deviation surrounding the mean and a maximum of half the mean value. In some cases, such as the catchability curve parameters, the standard deviation was determined to be too restrictive and was weakened accordingly. In runs where either the size spectrum or the catchability curve were kept constant, the standard deviations were set to 0. Values for which no priors were found within the literature were kept as a uniform distribution.

Estimated model parameters were allowed to vary from year to year, with priors on annual parameter estimates assigned using hierarchical normally distributed priors. That is, any given parameter λ_i in a given year, I was assigned a hierarchical random effect prior:

$$\lambda_i \sim Normal\,(\mu_\lambda, \sigma_\lambda)\,. \quad (6)$$

The global mean for each parameter (μ_λ) was in turn assigned either a normally distributed prior distribution with a mean from prior literature (an informative prior; Gelman et al. 2004), an exponential prior in the case of maximum size, or a uniform (uninformative) prior distribution if no prior information was available. All parameters were given bounds determined by biologically possible maxima and minima. The maximum size was given an exponential prior as we do not believe that Greenland Halibut in this study region are unlikely to reach the maximum size observed over the entirety of their distribution. Therefore, the likelihood was set highest at the maximum observed size across all survey years and decreasing to the maximum observed size ever recorded for Greenland Halibut. This prior was kept fairly tight as while it is likely there are bigger fish than has been observed in two decades of survey data, we don't anticipate that they would reach a size much larger. The standard deviations for the priors for global means were obtained provided from the literature whenever possible. If no variance value were available, a standard deviation representing the range of values found in other fish species was used (e.g. reported values for r in fish will range from 0.75 to 1 (e.g. Xiaojun and Ruyung 1990), and therefore a standard deviation of 0.25 was chosen for this parameter). In the situation where no standard deviations were available yet a mean value was found, as was the case with the parameter s, a weak prior global standard deviation was chosen. The standard deviations of the parameter random effects were assigned half-normal distributions (i.e. a zero-centered normal distribution, constrained to be >0). The values of the yearly parameter values were also constrained to satisfy theoretical limits on the values they could take (e.g. maximum possible length has to be equal to or larger than the biggest fish observed in the data set). All prior parameters, constraints, and

sources for means of priors for the global parameters are listed in Table 1. Priors for single-species size spectrum parameters were calculated from Andersen and Beyer (2006), catchability curve parameters from Harley et al. (2001), and maximum size information from Møller et al. (2018).

We used a total of four chains consisting of 10 000 iterations per chain, with a burn-in of 500 iterations to calibrate HMC tuning parameters, for each Stan model estimated (Hoffman and Gelman 2011). We assessed whether the models had converged to the posterior distribution by the end of the simulation following best practices recommended for Bayesian HMC models (Vehtari et al. 2021). We determined whether all parameters $\hat{r}$ values were <1.05 ($\hat{r}$ is a convergence diagnostic that compares between- and within-chain parameter estimates for each parameter, and should approach one in a convergent model), the effective sample size was over 1000, and the number of divergent transitions was low. We initially compared models with simply an increasing logistic catchability curve (i.e. $\beta_2 = 0$) but found that the inclusion of the uncatchable curve improved model fit: any model that did not include an uncatchable curve component was not able to model the observed rapid decline in catch with length observed in the data. As such, all results are from models estimated including an uncatchable curve.

As the catchability parameters are subject to a wide variety of potentially confounding environmental factors, and the size-spectrum parameters may be influenced by environmental conditions as well as finishing intensity, we allowed all the parameters to vary from year to year. Gaussian (random effect) priors were imposed on yearly variation for all catchability parameters except the size-spectrum scaling parameter and γ_2, both of which were kept uniform as no prior information was available to inform suitable priors (Table 1).

Model comparison

The model we constructed above was constructed from two individual model components, both of which were allowed to vary by year. In order to assess whether allowing annual variability in the parameters improved the overall fit of the model to the data, we compared four versions of the model: (a) the full model as was described above; (b) a version of the model where the size-spectrum parameters were fixed and the catchability curve parameters were allowed to vary across time; (c) a version of the model where the catchability curve parameters were fixed and the size-spectrum parameters were allowed to vary across time; and (d) a model where all parameters were constant across time. A leave-one-out cross-validation to determine the difference in their relative predictive accuracy was then conducted using the loo package in R (Vehtari et al. 2017). ELPD values, the theoretical expected log pointwise predictive density for a new dataset, were obtained for each model and compared to determine the model with the greatest predictive accuracy. The standard error of the difference in ELPD was also calculated to assess uncertainty in the difference in ELPD values.

Simulation trials

To assess the ability of the proposed model to accurately predict the true parameters defining a system as well as to assess the potential influence of sample size on the outcome, we constructed a simulated data set based on the mean parameter values for the model fit to all years of observed data. From this simulated data, we randomly sampled subsamples of 100, 250, 500, 1000, and 10 000 individuals. For each of these subsamples, the model was fit using 10 000 iterations and 4 chains to ensure convergence as indicated by $\hat{r} < 1.05$ for all parameters and effective sample sizes over 1000.

Results

Trawl data

The data underlying this article were provided by Fisheries and Oceans Canada by permission. Data will be shared on request to the corresponding author with permission of the relevant contacts at Fisheries and Oceans Canada. Over the 15 years of sampling, 1 397 trawls were conducted, with a mean and standard deviation of 93 and 43.2 sets per year, respectively. A total of 145 895 Greenland Halibut were sampled, with an average of 9 735 individuals caught per year and a standard deviation of 5 102 individuals per year. The sizes of Greenland Halibut ranged from 15 to 101 cm with the average size being 42 cm across all years.

Model results

The proposed model was found to converge for the 15 years of analyzed data (Appendix 2 available in Supplementary material). In order to remove divergent transitions, which were initially present (Appendix 3 available in Supplementary material), the adapt delta was increased from the default 0.9 to a value of 0.95, thereby reducing the step size, and the max tree depth from 10 to 12, increasing the number of nodes in the binary tree size within stan from 1024 to 4096 (Stan Development Team 2022). An effective sample size of at least 1000 was achieved for each parameter estimate and all $\hat{r}$ values were <1.005 if not exactly 1 (Table 2). If we analyze the model fit for 2019, e.g. we observe that the model not only converged but appears to suitably describe the variability i.e. observed in the data (Fig. 3, Table 2). The posterior mean often overestimates the number of small Greenland Halibut that would be caught by the net, likely a function of the size spectrum increasing faster than the catchability curve can account for. Furthermore, there were several observed groups of outliers associated with individual year classes from the estimated curve at ~20, 32, 37, and 51 cm (Fig. 3).

Variation in parameters over time

The model was run for the years 1999–2019, resulting in 15 years of data, considering there were several years where surveys were not conducted or where the survey was restricted to regions that made it incomparable to other years. None of the size spectrum parameters showed any substantive linear trend across the study period (Fig. 4), although estimates of the s parameter, representing the ratio of mortality rate to food assimilation rate, did vary substantially from year to year, relative to within-year posterior parameter variance (Fig. 4). We also observed a decreasing trend in the α_1 and an increasing trend in the α_2 (Fig. 4e and g). These changes correspond to potential shifts in the mid-points of the catchability curves over time. As a result, the size associated with peak of the observed distribution, a result of the model, was found to increase over the time period (Fig. 4i). It should be noted, however, that the model allowing for interannual variability among parameters was not supported as an improvement over the model where the parameters were not allowed to vary over time, suggest-

Table 2. Example posterior means, posterior standard deviations, and $\hat{r}$ values for estimated parameters for the model fitted to 2019 data.

Parameter	Posterior mean	95% credible interval	Bulk effective sample size	R-hat
r	0.853	0.580–1.077	2337	1.003
Δr	0.255	0.048–0.451	1525	1.003
s	0.566	0.242–0.897	2861	1.001
m_∞	30 061 g	15 855–42 875 g	3678	1.001
γ_2	0.003	0.001–0.008	2679	1.000
α_1	8.818	7.538–10.191	3878	1.001
β_1	0.187	0.135–0.241	4698	1.001
α_2	11.493	8.204–16.224	1645	1.000
β_2	0.222	0.174–0.283	1763	1.000

The year 2019 was chosen as a representative year, being the closest year to the year this study was conducted. For fits for other years, see Appendix 2 available in Supplementary material.

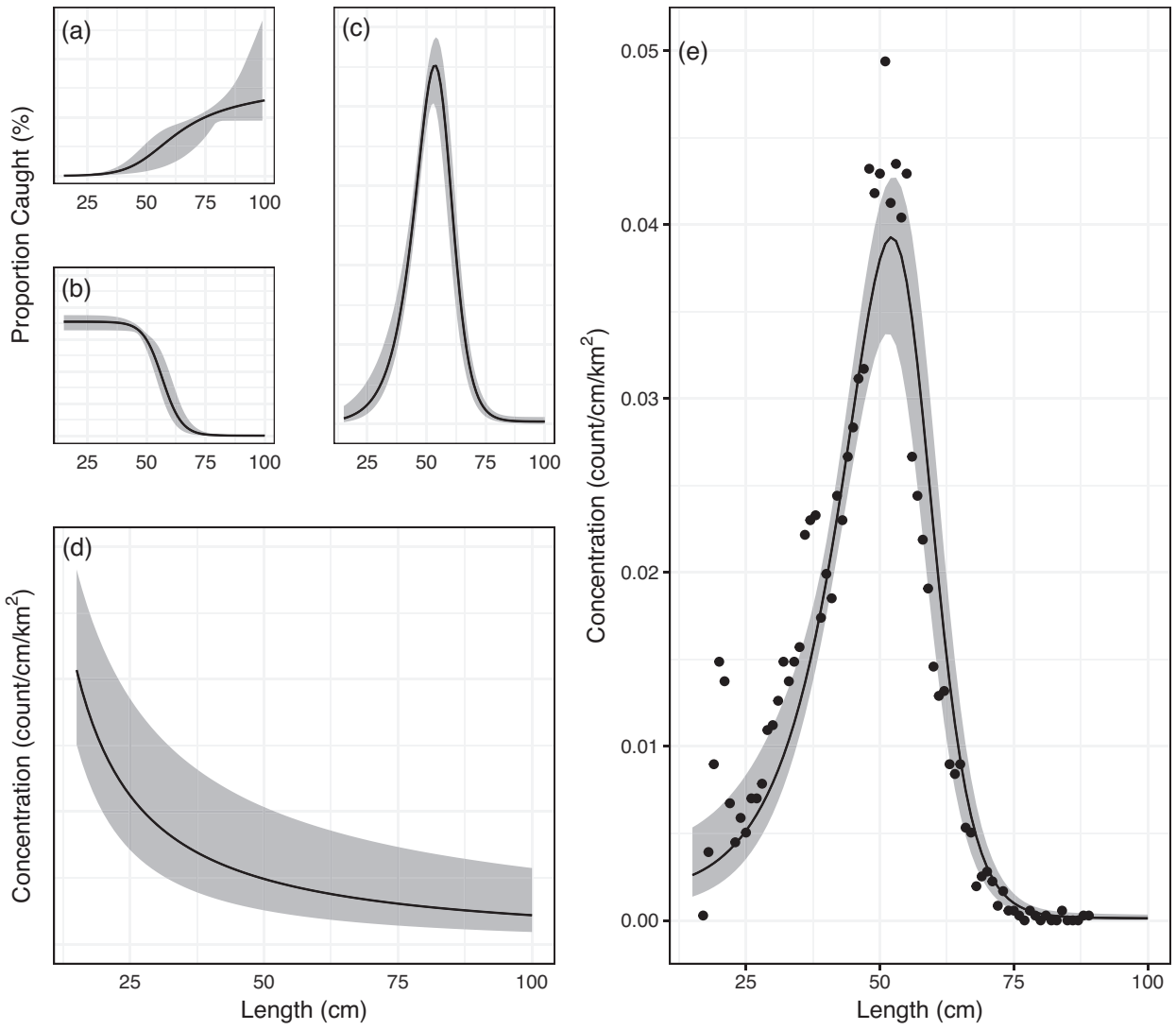

Figure 3. Sample fit of our model to length data collected for Greenland Halibut on the Nunavut shelf in 2019. (a)–(d) represent fitted curves for the three components of the model: (a) the ascending catchability curve; (b) the left-hand descending catchability curve; (c) the combined selectivity curves; and (d) the single species size spectrum. These components combine to form (e): the product of the three component curves, rescaled to sum to one to show the predicted fraction of total catch occurring in each size bin. The points represent the observed fraction of total counts for each 1 cm size category. Solid black lines represent the posterior mean. The grey bands represent 95% credible intervals.

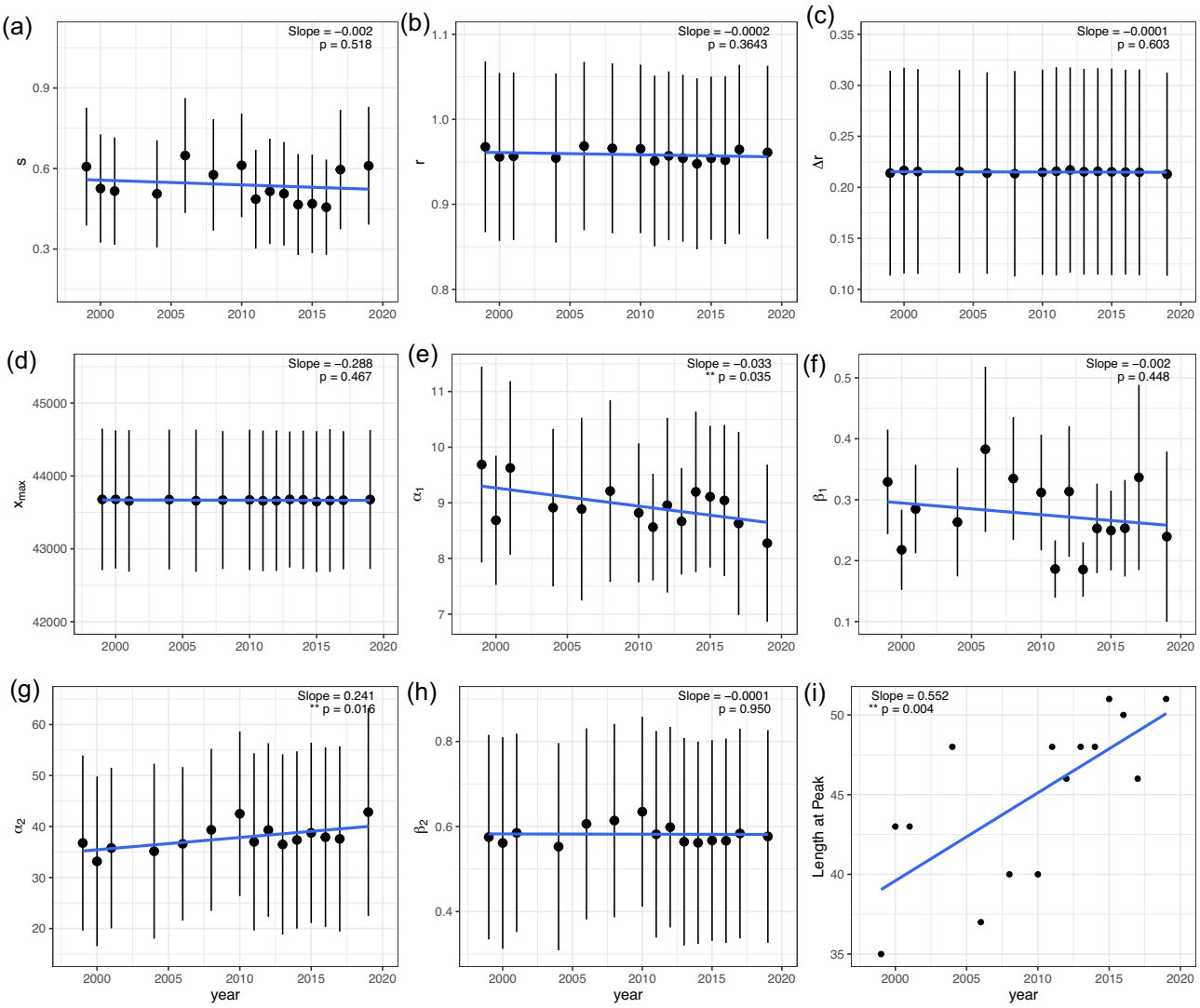

Figure 4. Trends in the model parameters over time. Panels a–d represent the parameters from the single-species size spectrum. Panels e–h represent the size-specific catchability and uncatchable parameters. In these panels, the points represent mean posterior draws and the black lines represent the standard deviation around these points. A blue trendline is also present with its slope and the *P*-value with the associated regression analysis shown. Panel i demonstrates, using points, the length associated with the location of the peak of the distribution with the blue line demonstrating the trend over time.

ing that this observed trend, though visible from the observed size distributions over time, were not well supported by the model.

Model comparison

ELPD, or the theoretical expected log pointwise predictive density, and standard error of the ELPD were estimated for each of the models (Table 3). As expected, the non-time-varying model performed the least well of the four analyzed models, followed by the fixed catchability, the full model, and the fixed size spectrum model performing the best of the four models. However, the standard errors associated with each of these models were equal to the difference in the ELPD from the base model, suggesting that there is only weak support for these time-varying models being an improvement over the non-time-varying alternative.

Simulation trials

Convergence was obtained for each of the sub-sample runs that were conducted (Table 4). While many of the parameters were reasonably approximated, the model struggles to estimate certain parameters. For example, the maximum size of the fish is often not well estimated, representing a size of fish far beyond the maximum observed size. The model therefore recognizes that the maximum size is a larger number, but struggles to identify where exactly the size spectrum is anticipated to quickly drop to 0. Similarly, the exact location where the curve drops off as part of the uncatchable curve was found to be difficult to approximate at lower sample sizes. While we did find that the exclusion of such a curve resulted in poor fits to the distribution (Appendix 4 available in Supplementary material), without sufficient data the model had difficulty determining where the drop in catchability should occur.

Table 3. Leave-one-out analysis for the four proposed models to assess the predictive capabilities of the varying components of the models to annual variability.

Model	Difference in ELPD from base model	SE of ELPD
All parameter fixed (base model)	0	0
Fixed catchability parameters	32 859.4	32 859.3
All parameters allowed to vary	540 781.5	540 781.5
Fixed size spectrum parameters	1 682 270.6	1 682 270.7

The ELPD for each model was compared to a base model consisting of non-time-varying components.

Table 4. Simulation trial estimates for various sub-sample sizes.

Variable	Subsample size					True value
	100	250	500	1 000	100 000	
Δr	Did not converge	0.20 ± 0.16	0.22 ± 0.13	0.25 ± 0.23	0.25 ± 0.14	0.22
r		0.95 ± 0.25	1.24 ± 0.19	1.04 ± 0.23	0.99 ± 0.21	0.96
s		0.49 ± 0.26	0.55 ± 0.27	0.49 ± 0.29	0.52 ± 0.29	0.61
m_∞		24 902 ± 9 847	28 250 ± 8 778	28 413 ± 9 102	40 650 ± 8 385	43 677
γ_2		0.03 ± 0.03	0.03 ± 0.03	0.02 ± 0.01	0.01 ± 0.00	0.01
α_1		8.20 ± 1.29	9.47 ± 0.62	8.61 ± 0.50	8.08 ± 0.09	8.14
β_1		0.29 ± 0.05	0.30 ± 0.02	0.29 ± 0.02	0.28 ± 0.00	0.28
α_2		63.8 ± 27.45	54.64 ± 9.43	51.97 ± 9.19	38.39 ± 1.37	37.77
β_2		0.62 ± 0.3	0.85 ± 0.14	0.60 ± 0.14	0.59 ± 0.02	0.58

Discussion

Given the wide range of factors contributing to the catchability of a given species, we sought to investigate whether we could estimate not only catchability parameters from trawl data, but also species-specific size spectra. The resulting model contained a total of 10 parameters that were estimated within a Bayesian framework. Furthermore, we analyzed 15 years of data, with every parameter being allowed to vary by year. A visual analysis of the resulting model revealed a reasonable fit to the distribution of sizes observed within a given year, suggesting the model not only converged, but also provided a reasonable representation for the general visible trends within the data (Appendix 2 available in Supplementary material).

We additionally asked the question: can we use this derived model to measure population changes in the Greenland Halibut in light of its expanding offshore fishery along the Nunavut shelf? We were unable to detect a trend in size spectrum parameters and, therefore, were unable to detect any impacts of fishing activities on the single-species size spectrum. However, we did observe a shift in the peak of the distributions. Although trends were found in the catchability and uncatchable curve parameters, which could explain this shift in the peak, the fact that the time-varying model was not found to perform better than a static one suggests that these trends are not strongly supported. This increased average of size of the catch is unlikely to be related to a large size class, e.g. as the growth of the species undoubtedly surpasses the observed slope of the relationship between the length at the peak and the year. It therefore seems likely that other factors, such as decreasing fish density, could be contributing to this general trend.

Variation in peak length over time

One of the observed trends was the increase in the location of the peak of the caught distribution of fish. With the removal of larger individuals, we had initially anticipated that the location of this peak would decrease over time. However, the reverse trend was observed. With regard to the parameters of the model, the only parameters that were found to vary substantively over time were the two α parameters associated with the catchability curves. Therefore, our model suggests that while the species-specific size spectrum has remained the same over the time period, it is the changes in catchability of the species that result in the observed shift in the peak. This could be due to either changes in the behavior of the fish, or shifts in the spatial distribution of the trawl survey, as the survey did not follow a spatially fixed sampling design across the study period.

We acknowledge other factors, not accounted for in our model, may have caused the change in the estimated peak length besides a change in catchability. For instance, the Andersen and Beyer model assumes non-varying recruitment. However, in the situation where recruitment was found to decrease over time, this could result in the observed shift in the peak of the observed distribution i.e. currently not adequately accounted for in the parameters. Published recruitment indices for the Greenland Halibut along the Nunavut shelf indicate little evidence for time-varying recruitment (Treble and Nogueira 2020), so this explanation does not seem likely to us. We also assume that the true population size spectrum in any given year matches the equilibrium size spectrum derived by Andersen and Beyer (2006), which can include the effects of fishing mortality; however, as those authors note, the equilibrium distribution assumes size-invariant fishing rates. Higher-than-expected mortality on larger fish (resulting in a steeper-than-expected right tail of the size spectrum) could result in an increase in the uncatchable curve in our model, as could higher-than-expected mortality on smaller fish, if large fish become more difficult to capture while fishing (resulting in an increased estimate of catchability of smaller fish). Similarly, if the rate of decrease for juveniles was higher than predicted, the model would attempt to account for this change by adjusting the catchability curve. If the change in peak length that we observed was caused by increased fishing pressure, rather than altered catchability, we predict that smaller Greenland

Halibut should be more vulnerable to fishing than large ones (as would be expected if large Greenland Halibut were able to sense and avoid fishing gear). We suggest that this could be testable via mark–recapture studies.

Effects of parameter correlation on estimates

We observed that several of the parameters were highly correlated with each other, namely the α and β components for the catchability curve as well as the uncatchable curve (Appendix 3 available in Supplementary material). As the midpoint of the catchability curve decreases, the model compensates for that by decreasing the steepness of the curve. A similar trend occurs in the uncatchable curve. This kind of correlation between estimated parameters is a standard feature of complex statistical models (Xu and Gertner 2008), and indicates that, under a given model specification, it may be difficult or impossible to estimate the most predictive value of each parameter individually; for instance, it is possible to get a very similar-shaped catchability curve with a high value of α_1 and high value of β_1 (corresponding to a low intercept and steep slope) or with a low value of α_1 and of β_1 (corresponding to a high intercept and shallow slope). However, our research question focused on estimating the overall shape of the three curves (Fig. 2), rather than precise estimates of specific parameters; as demonstrated by Fig. 3, the resulting curves are estimated with high precision, even if the individual parameters are not.

Evidence for the declining catchability with size of Greenland Halibut

Most catchability studies simply consider the increasing logistic function to describe the catchability curve for a given species. For many species that do not reach large sizes, such as many forage fish species, this statement is appropriate as the maximum size of the species falls on the increasing slope of the catchability curve. Other authors, however, have noted an apparent asymmetric dome-shaped catchability curve with several study species (Hoydal et al. 1982, Fraser et al. 2007).

We consider our results to provide strong evidence for declining catchability with size in Greenland Halibut. If we excluded the uncatchable curve, our model frequently exhibited poor convergence (a sign of poor statistical fit to the data) and even when it did converge, the fitted model always overestimated the number of large individuals present within the catch (Appendix 4 available in Supplementary material). The observed rapid decline in catch with size could only occur due to population dynamics alone if Greenland Halibut either stopped growing more quickly, or died at much higher rates at larger sizes than assumed by the Andersen and Beyer model. The first can be ruled out based on prior studies of growth in this species (Bowering and Nedreaas 2001), and we know of no evidence for increasing mortality with age or size in Greenland Halibut.

Decreasing catchability with increased size may occur due to increased swimming endurance, and therefore their ability to outswim or otherwise evade a trawl will increase with increased size (Videler and Wardle 1991, He 1993, Winger et al. 1999, Krag et al. 2014). Furthermore, as fishing practices continue, it has been proposed that, as we are repeatedly removing the slower fish, that we are unintentionally driving the evolution of wild fish populations to favor individuals with a greater capacity for anaerobic metabolism (Killen et al. 2015). The potential for a species to become uncatchable will influence the observed distribution of sizes will increase as human exploitation of fish stocks continues. The assumption that once a species reaches maximum catchability, it will retain that degree of catchability across all sizes is questionable, and therefore considerations should be made regarding the catchability as a species approaches maximum size. However, in the case of the scenario where a given species has a sufficiently high α_2/β_2 ratio (representing the midpoint of the uncatchable curve), near or above the maximum size of a given species, the parameter would have little impact on the outcome of the model. In this case, the model could be further simplified by removing the uncatchable curve from the equation, reducing it to the product of a single-species size spectrum and an ascending catchability curve. The escapement of larger individuals has been suggested in a number of studies. Paired trawl experiments found that not only do we observe a decreased catchability of large fish, but that the magnitude of this decrease was influenced by the mesh size of the gear (Mous et al. 2002, Krag et al. 2014, Weinberg et al. 2016). This finding suggests that the fish were not only able to escape the trawl, but that their efficiency at doing so was influenced by gear selection. Video recordings of Greenland Halibut response to a trawl has shown that many individuals will simply lay close to the bottom, thereby escaping beneath the trawl, and that large individuals in particular often will escape ahead of the trawl by swimming horizontally out of the path of the trawl (Albert et al. 2003, 2006). The inclusion of the uncatchable curve is not only necessary from a modeling perspective but also supported by the behaviors of this species.

Relative vs. absolute catchability

This analysis has focused on estimating the relative catchability of the species. The parameter γ_1 (representing the maximum catchability) was therefore set to one for all years and trawls. The exact value of γ_1 for the absolute catchability of the species cannot be determined from the catch data alone. This value is most likely to be <1 to account for the percentage of fish to evade the net. However, values >1 have been reported on account of potential herding of some species of fish into the net (Somerton 1996, Fraser et al. 2007, Bryan et al. 2014). Frequently, the potentially trawled biomass is determined through the use of acoustic data (e.g. Edwards 1968, Sissenwine and Bowman 1978, Harley and Myers 2001). As such, the parameter γ_1 will therefore need to be estimated using alternative approaches. However, variation in relative catchability due to known environmental factors, such as day–night variation, can be estimated by comparing trawls taken close in time and space, but varying in key parameters. Based on comparisons of abundance of nighttime and daytime trawls, we determined that there was limited evidence of diel variation in catchability of Greenland Halibut (see Appendix 5 available in Supplementary material).

Single-species size spectrum

Although this study did not find any long-term changes in the single-species size spectrum parameters over the analyzed 20-year period, the potential of fluctuations in the various parameters could indicate a number of things relating to the

biology of the species. The parameter Δr is the exponent of the relationship of mass to the basic energy requirements for growth and maintenance (Rubner 1883, Brody and Lardy 1946, West et al. 1997) relative to the parameter r, the exponent of the relationship between mass and the standard metabolic rate (SMR; Krogh 1914, West et al. 2001). Variation in these parameters would indicate changes in the energy requirements of the species, such as those induced by changing ocean conditions (Johnston and Dunn 1987, Clarke and Johnston 1999) or increased energy investiture in the pursuit of prey, or to avoid predation (Seibel and Drazen 2007). The parameter complex s represents the ratio of predation to the rate of food assimilation. Increased fishing activity is expected to increase this ratio, as we remove greater quantities of fish from the community as fishing increases. Alternatively, if food was becoming scarce, we might expect this ratio to decrease, possibly associated with a decrease in the parameter Δr to indicate a decrease in foraging efficiency, or an increase in natural predation for which we presently do not have evidence for. The final term of the size spectrum equation is the maximum size of the fish. One of the key indicators of the negative impacts of fishing is the reduction of the maximum size of the species resulting from the preferential removal of larger individuals (Hsieh et al. 2010, Heino et al. 2015). Much as the catchability of a given species is expected to vary with season, the size spectrum is anticipated to vary over the course of the year. The size spectra presented here represent what we would observe in the region during the late summer and early fall, when the surveys take place. It is expected that varying surrounding temperatures will significantly influence the SMR of members of these communities (Fry 1971), food assimilation rates (Ricker 1946, Andersen 1999), and growth (Pauly 1980, Fonds et al. 1992, King et al. 1999). Without even considering confounding factors such as seasonal variability in prey availability, we would expect the size spectrum parameters r, Δr, and s to vary with water temperature.

For the construction of our model, the parameter estimates are kept constant across the size range of fish. This approach is reasonable for the parameters representing the relationship between the mass and energy requirements of the fish (n and r), as well as the maximum size of the species, but the parameter that could be impacted by this decision is s, representing the ratio of mortality to food assimilation. It has been shown that many marine fish species experience age-specific mortality (Lorenzen 2000, Gislason et al. 2010, Thorson and Prager 2011). However, we do not presently have methods to account for the potential of variation in mortality with size with our data set, and therefore the parameter s was kept constant such that the descending slope of the size spectrum only significantly deviated from a near log-linear relationship as the species approached maximum size. Furthermore, the Andersen and Beyer model was generated with the caveat that fishing mortality was not included in their model. We had assumed that an increase in fishing mortality would be reflected in the parameter s. If the Andersen and Beyer model, however, is too rigid of a model to detect the influence of size-specific fishing mortality on the population, it might instead attempt to ascribe the variation to the catchability curve. If this scenario were the case, the changes in size-spectrum parameters over time would have erroneously been attributed to changes in the catchability parameters. If the parameter s was assumed to be constant when in fact there was increased mortality, either natural or due to fishing, we would anticipate observing a steepening of the descending slope, which the model would explain through the two β parameters associated with the steepness of the catchability curves. The changing of these parameters would allow for the more rapid decline of the right-hand descending slope and allow the left-hand curve to accommodate the now increased predicted numbers at lower sizes. Instead, both of these are found to be constant over time and that the α values are found to change, indicating the midpoint of these catchability curves is changing given a constant β. Future studies could help shed light on the impacts of keeping this parameter s constant by determining the impact of varying mortality with size on single-species size spectra.

Systematic patterns of residual variation around predicted size spectrum

While the model captures the peak of the distribution and provides an approximation of the ascending and descending slope, observed catches differed systematically from the overall trend in several years (e.g. higher-than-expected counts of fish near 25 and 50 cm in 2019; Fig. 3d). One possible cause for these would be annual recruitment pulses moving through the size spectrum. The species-specific size spectrum in Equation (1) that we assumed was derived from a steady-state population model, where recruitment occurs continuously throughout the year, and temporal variation in recruitment, mortality, or growth is absent (Andersen and Beyer 2006). Reproduction in Greenland Halibut, on the other hand, is seasonal (Gundersen et al. 2010).

The presence of detectable year classes could bias our parameter estimates for some years. For example, should a particularly strong year class arise for a given species, the model will interpret this deviation as the peak of the distribution and, as a result, will produce erroneous conclusions when attempting to fit catchability curves and single-species size spectra. In the absence of a seasonally driven size-spectrum model to compare our results to, it is difficult to assess the impact of recruitment pulses on our estimated size spectra. We suggest that a useful area of future study in the theory of size spectra would be to extend the steady-state size spectrum solutions from Andersen and Beyer (2006) to determine size spectra for fish species with seasonal reproduction. We hypothesize that the resulting size spectrum should be similar in shape to the spectrum predicted by Andersen and Beyer, but with additional local peaks corresponding to the average size of age-0, 1, 2, etc. fish at the time of sampling.

We also observed that, while our model was able to consistently estimate the location of the peak of the observed size distribution across years, as well as the general pattern of the ascending and descending slopes, our model systematically underestimated the height and sharpness of the observed peak of the observed size distribution. The model appears incapable of achieving the sharp peak that we observe in the data without compromising the fit to the remainder of the data (e.g. see Fig. 3d). This discrepancy may also be due to the pulsed effect of seasonal reproduction. However, it may also indicate a potential issue with the assumed functional shapes of the catchable and/or uncatchable curves (i.e. one or both of these curves may change more rapidly than is possible under our assumed logistic curves).

Effects of the assumed minimum fish size and the shape of the catchability curve

The single-species size spectrum from Andersen and Beyer (2006) requires that the minimum size of fish possible is >0; otherwise, the size spectrum would not integrate to any finite value. To use our method, this minimum size needs to be either estimated or specified by the user. We chose a minimum length equal to the smallest size fish observed in the survey for this study. This was in part because we did not have good ecological information on the smallest size of Greenland Halibut at this time of year.

We suspect that the actual smallest size classes of Greenland Halibut are smaller than the observed 15 cm minimum. We think this model sensitivity may highlight an issue with the assumed logistic catchability curve. The curve predicts that catchability at small sizes will be approximately $e^{\alpha_l+\beta_l l_{min}}$, which will always be >0. In reality, instead of the catchability curve approaching 0 as the length approaches 0, there will likely be a length >0 where the catchability will be 0, as fish much smaller than the net mesh are likely to pass easily through the net. This is evidenced by the fact that larval fish are rarely caught in otter trawls, despite their relative abundance within a given ecosystem. Eventually, the fish will be too small to be caught within a net of a given mesh size to any reasonable capacity. Much as two of the source models do not realistically describe the activity of the curves as they approach length/mass of 0, it comes as no surprise that our model also produces unrealistic expectations. As a result, a cut-off needs to be set at the discretion of the author to ensure reliable curve fitting.

For the creation of this model, we had selected a catchability curve that was comprised of the combination of two curves, allowing for a wide variety of potential shapes. If, e.g. the investigator were to find that α_2 were to be quite large, approaching or even exceeding the maximum size observed, that would be justification for simplifying this component of the model to simply an ascending asymptotic catchability curve. Similarly, as certain parameter combination exist that would justify a dome-shaped selectivity, the model may be similarly simplified to accommodate this additional prior information on the behavior of a target species. Equation (3) could also be substituted for a wide variety of catchability curves and thereby the investigator need not be limited to a catchability-uncatchable curve function to describe their population.

Potential effects of spatial population structure, sample size, and changing environmental conditions on estimated parameters

The single-species size spectrum assumes that the sample is representative of an entire well-mixed population, with little to no spatial separation of individuals from different life stages. The model still will describe the observed distribution as long as the trawl survey includes reasonable coverage of the whole range of a population. However, if a trawl survey only samples juveniles or spawning adults, this will result in a bias with regard to both the catchability and the size spectra parameters. It is therefore important to have a general understanding of the population and to visualize the data prior to fitting the model to ensure proper interpretation of the results. Furthermore, the sample size needs to be sufficiently large in order for the model to adequately describe the population it was taken from. Simulating novel data from this model with varying sample sizes indicated at least 500 individuals were required per year for the model to consistently converge (Appendix 6 available in Supplementary material)). These simulations also indicated that it is not possible to reliably estimate the true maximum size (x_{max}); the posterior mean value of x_{max} for 2019 varied substantially among subsamples, ranging from 30 to 44 kg. This is likely because the maximum size of the fish represents a size larger than the biggest size class in the observed size distribution, so there is limited data in the sample on where this maxima occurs. In addition to the parameters existing in the present model, there are other potential factors that could influence the shape of a single-species size spectrum. First, the single-species size spectrum equation was created to describe an entire population. However, trawl data only provides a glimpse at what was available at a given location. If, e.g. individuals of different ages/size classes do not occupy the same areas, misleading model results could arise. Evidence exists that juvenile Greenland Halibut of sizes that would comprise the underrepresented lower portion (<35 cm) of the distribution may occupy a different spatial location than larger individuals (Albert 2003, Wheeland and Morgan 2020, Gíslason et al. 2023). To reduce bias associated with this observation, we did not include sets that targeted these juvenile-occupied areas in our study, as these locations were not included in surveys every year. The implications of this action are that the left end of the fit curve was potentially lower than that of the entirety of the population along the shelf and the catchability parameters might have changed slightly with their inclusion despite the fact that the majority of the points defining the ascending catchability curve would not be influenced by this decision.

A final major factor that was not accounted for in this study is changing environmental conditions. Of particular concern in the Arctic are the influences of climate change on natural ecosystems. Over the past 100 years, the Arctic has observed a 1.5° increase in air temperatures though water temperatures in the northern North Atlantic appear to have been relatively stable thus far (ACIA 2005). Anticipated future changes to the Arctic marine environment include changes in community composition from distribution shifts (Perry et al. 2005, Cheung et al. 2009), negative impacts of UV radiation (El-Sayed et al. 1996, Zagarese and Williamson 2001, Alves and Agustí 2020), changes in sea ice coverage (Johannessen et al. 2004, Comiso and Hall 2014), dispersal ability (Lett et al. 2010), wind-driven patterns influencing larval fish production and survival (Hollowed et al. 2009, Lacroix et al. 2017), and growth rates (King et al. 1999, Denechaud et al. 2020). Furthermore, the impacts of fishing activities on fish populations have been proposed to make these populations more sensitive to additional pressures imposed by climate change (Ottersen et al. 2006, Brander 2007). Many of these factors are anticipated to potentially influence the single-species size spectrum for a given species. Although we did not observe any long-term trends in the life history parameters in our analyzed size spectra, these considerations should be taken into consideration before assuming that any observed change is directly related to fisheries.

Summary

This study was initially inspired by the large degree of uncertainty in using published size-specific catchability curves, given the wide variety of factors that have been shown to

influence these curves. By combining the theory behind size-based catchability with size spectrum theory, we have created a model that reasonably describes the variation observed in the data, and is capable of estimating both size spectra and catchability curves from a single survey. The parameter estimation does not depend on specialized study designs, such as pairing catch data with acoustic data, nor does it require multiple years of size data, which, e.g. may be used to implement virtual population analysis. This model therefore represents an adaptive framework that can be applied to any observed distribution of sizes for a given species from trawl data, assuming sufficient sample sizes, thereby removing the assumptions that the catchabilities in a given study will be comparable to previously published studies. Furthermore, this analysis allows for the estimation of catchability parameters for species where more extensive studies have not been conducted.

Acknowledgements

We asked Margaret Treble and Kevin Hedges at the Fisheries and Oceans Canada for access to the Greenland Halibut trawl survey data, which was input into this model. We also would like to thank Guillaume Blanchet for feedback on our modeling approach, and Valentin Lucet with help with debugging code issues. Finally, we thank the various members of the Pedersen Quantitative Ecology Lab (Natalie Dupont, Fonya Irvine, Danielle MacRae, Alexander Schade, Spencer Schurman, Allegra Spensieri, Alienor Stahl, and John-Philip Williams) for their insightful comments on the work.

Supplementary data

Supplementary data is available at *ICESJM Journal* online.

Conflict of interest: The authors have no conflict of interest to declare.

Data availability

The data underlying this article were provided by Fisheries and Oceans Canada by permission. Data may be shared on request to the corresponding author with permission of Margret Treble and/or Kevin Hedes of Fisheries and Oceans Canada.

Author contributions

K. Krumsick was responsible for project conceptualization, funding acquisition, project administration, methodology, data analysis, including R coding, and production of the original draft of this manuscript. E. Pedersen was responsible for aiding in project development, supervision, and contributed to manuscript writing and revisions.

Funding

This project was funded as part of a Mitacs Accelerate fellowship working with industry partner Brian Burke of the Nunavut Fisheries Association, with additional funding from the NSERC Discovery Grant program.

References

ACIA (Arctic Climate Impact Assessment). *Arctic Climate Impact Assessment: Scientific Report*. Cambridge: Cambridge University Press, 2005, 1042.

Albert OT, Harbitz A, Høines ÅS. Greenland Halibut observed by video in front of survey trawl: behaviour, escapement, and spatial patter. *J Sea Res* 2003;**50**:117–27. https://doi.org/10.1016/S1385-1101(03)00063-7

Albert OT, Salberg A-B, Zaferman M *et al*. Effects of artificial light on trawl catch and behaviour of Greenland halibut in front of trawls. *Deep Sea 2003: Conference Poster Papers and Workshop Papers* 2006;**2**:142–146.

Albert OT. Migration from nursery to spawning area in relation to growth and maturation of Greenland halibut (*Reinhardtius hippoglossoides*) in the northeast Arctic. *J Northw Atl Fish Sci* 2003;**31**:113–25. https://doi.org/10.2960/J.v31.a8

Alves RN, Agustí S. Effect of ultraviolet radiation (UVR) on the life stages of fish. *Rev Fish Biol Fish* 2020;**30**:335–72. https://doi.org/10.1007/s11160-020-09603-1

Andersen KH, Beyer JE. Asymptotic size determines species abundance in the marine size spectrum. *Am Nat* 2006;**168**:54–61. https://doi.org/10.1086/504849

Andersen KH, Pedersen M. Damped trophic cascades driven by fishing in model marine ecosystems. *Proc R Soc B Biol Sci* 2009;**227**:795–802.

Andersen NG. The effect of predator size, temperature and prey characteristics on gastric evacuation in whiting. *J Fish Biol* 1999;**54**:287–301. https://doi.org/10.1111/j.1095-8649.1999.tb00830.x

Arreguín-Sánchez F. Catchability: a key parameter for fish stock assessment. *Rev Fish Biol Fish* 1996;**6**:221–42. https://doi.org/10.1007/BF00182344

Barange M, Pillar SC, Huse I *et al*. Vertical migration, catchability and acoustic assessment of semi-pelagic Cape horse mackerel *Trachurus trachurus* capensis in the southern Benguela. *Afr J Mar Sci* 2005;**27**:459–69. https://doi.org/10.2989/18142320509504104

Benoît HP, Swain DP. Accounting for length- and depth-dependent diel variation in catchability of fish and invertebrates in an annual bottom-trawl survey. *ICES J Mar Sci* 2003;**60**:1298–317. https://doi.org/10.1016/S1054-3139(03)00124-3

Blanchard JL, Jennings S, Law R *et al*. How does abundance scale with body size in coupled size-structured food webs? *J Anim Ecol* 2009;**78**:270–80. https://doi.org/10.1111/j.1365-2656.2008.01466.x

Bowering WR, Nedreaas KH. Age validation and growth of Greenland halibut (*Reinhardtius hippoglossoides* (Walbaum)): a comparison of populations in the northwest and northeast Atlantic. *Sarsia* 2001;**86**:53–68. https://doi.org/10.1080/00364827.2001.10420461

Brander KM. Global fish production and climate change. *Proc Nat Acad Sci* 2007;**104**:19709–14. https://doi.org/10.1073/pnas.0702059104

Brody S, Lardy HA. Bioenergetics and growth. *J Phys Chem* 1946;**50**:168–9. https://doi.org/10.1021/j150446a008

Brodziak JK, Legault CM, Col LA *et al*. Estimation of demersal and pelagic species biomasses in the northeast USA continental shelf ecosystem. *ICES CM* 2004;**7**:42.

Bryan DR, Bosley KL, Hicks AC *et al*. Quantitative video analysis of flatfish herding behavior and impact on effective area swept of a survey trawl. *Fish Res* 2014;**154**:120–6. https://doi.org/10.1016/j.fishres.2014.02.007

Cadigan NG, Walsh SJ, Brodie W. Relative efficiency of the *Wilfred Templeman* and *Alfred Needler* research vessels using a Campelen 1800 shrimp trawl in NAFO subdivision 3Ps and divisions 3LN. *CSAS Res Doc* 2006;**85**:1–59.

Chen J, Thompson ME, Wu C. Estimation of fish abundance indices based on scientific research trawl surveys. *Biometrics* 2004;**60**:116–23. https://doi.org/10.1111/j.0006-341X.2004.00162.x

Cheung WWL, Lam VWY, Sarmiento JL *et al*. Projecting global marine biodiversity impacts under climate change scenarios. *Fish Fish*

2009;**10**:235–51. https://doi.org/10.1111/j.1467-2979.2008.00315.x

Chongliang Z, Chen Y, Thomspon K *et al.* Implementing a multispecies size-spectrum model in a data-poor ecosystem. *Acta Oceanolog Sin* 2016;**35**:63–73.

Clarke A, Johnston NM. Scaling of metabolic rate with body mass and temperature in teleost fish. *J Anim Ecol* 1999;**68**:893–905. https://doi.org/10.1046/j.1365-2656.1999.00337.x

Coad BW, Reist JD. *Marine Fishes of Arctic Canada*. Toronto: University of Toronto Press, 2018.

Comiso JC, Hall DK. Climate trends in the Arctic as observed from space. *Wiley Interdiscip Rev Clim Change* 2014;**5**:389–409. https://doi.org/10.1002/wcc.277

Daan N, Gislason H, Pope JG *et al.* Changes in the North Sea fish community: evidence of indirect effects of fishing? *ICES J Mar Sci* 2005;**62**:177–88. https://doi.org/10.1016/j.icesjms.2004.08.020

Denechaud C, Smoliński S, Geffen AJ *et al.* A century of fish growth in relation to climate change, population dynamics and exploitation. *Global Change Biol* 2020;**26**:5661–78. https://doi.org/10.1111/gcb.15298

Dremière P-Y, Fiorentini L, Cosimi G *et al.* Escapement from the main body of the bottom trawl used for the Mediterranean international trawl survey (MEDITS). *Aquat Living Resour* 1999;**12**:207–17. https://doi.org/10.1016/S0990-7440(00)88471-5

Edwards AM, Robinson JP, Plank MJ *et al.* Testing and recommending methods for fitting size spectra to data. *Methods Ecol Evol* 2017;**8**:57–67. https://doi.org/10.1111/2041-210X.12641

Edwards RL. Fishery Resources of the North Atlantic Area. In: D. W. Gilbert (ed.), *The Future of the Fishing Industry of the United States*. Washington: University of Washington, 1968, 52–60.

El-Sayed SZ, Van Dijken GL, Gonzales-Rodas G. Effect of ultraviolet radiation on marine ecosystems. *Int J Environ Stud* 1996;**51**:199–216. https://doi.org/10.1080/00207239608711081

Engås A, Godø OR. Escape of fish under the fishing line of a Norwegian sampling trawl and its influence on survey results. *ICES J Mar Sci* 1989;**45**:269–76. https://doi.org/10.1093/icesjms/45.3.269

Engås A, Godø OR. Influence of trawl geometry and vertical distribution of fish on sampling with bottom trawl. *J Northw Atl Fish Sci* 1986;**7**:35–42. https://doi.org/10.2960/J.v7.a4

Fonds M, Cronie R, Vethaak AD *et al.* Metabolism, food consumption and growth of plaice (*Pleuronectes platessa*) and flounder (*Platichthys flesus*) in relation to fish size and temperature. *Neth J Sea Res* 1992;**29**:127–43. https://doi.org/10.1016/0077-7579(92)90014-6

Fraser HM, Greenstreet SPR, Piet GJ. Taking account of catchability in groundfish survey trawls: implications for estimating demersal fish biomass. *ICES J Mar Sci* 2007;**64**:1800–19. https://doi.org/10.1093/icesjms/fsm145

Fry FEJ. The effect of environmental factors on phsiology of fish. *Fish Physiol* 1971;**6**: 1–98. https://doi.org/10.1016/S1546-5098(08)60146-6

Gabr M, Fujimori Y, Shimizu S *et al.* Behaviour analysis of undersized fish escaping through square meshes and separating grids in simulated trawling experiment. *Fish Res* 2007;**85**:112–21. https://doi.org/10.1016/j.fishres.2007.01.006

Gelman A, Carlin JB, Stern HS *et al. Bayesian Data Analysis*, 2nd edn. New York, NY: Tests in Statistical Scence, 2004.

Gíslason D, Estévez-Barcia D, Sveinsson S *et al.* Population structure discovered in juveniles of Greenland halibut (*Reinhardtius hippoglossoides* Walbaum, 1792). *ICES J Mar Sci* 2023; **80**: 889–96.

Gislason H, Daan N, Rice JC *et al.* Size, growth, temperature and the natural mortality of marine fish. *Fish Fish* 2010;**11**:149–58. https://doi.org/10.1111/j.1467-2979.2009.00350.x

Godø OR, Walsh SJ, Engås A. Investigating density-dependent catchability in bottom-trawl surveys. *ICES J Mar Sci* 1999;**56**:292–8. https://doi.org/10.1006/jmsc.1999.0444

Gordoa A, Masó M, Voges L. Monthly variability in the catchability of Namibian hake and its relationship with environmental seasonality. *Fish Res* 2000;**48**:185–95. https://doi.org/10.1016/S0165-7836(00)00160-0

Government of Nunavut. 2016. Nunavut fisheries strategy: 2016–2020. 50pp. Available from: https://assembly.nu.ca/sites/default/files/TD-277-4(3)-EN-Department-of-Environment's-Nunavut-Fisheries-Strategy,-2016-2020.pdf (28 July 2022, date last accessed).

Gundersen AC, Stenberg C, Fossen I *et al.* Sexual maturity cycle and spawning of Greenland halibut *Reinhardtius hippoglossoides* in the Davis Strait. *J Fish Biol* 2010;**77**:211–26. https://doi.org/10.1111/j.1095-8649.2010.02671.x

Harley SJ, Myers R, Barrowman N *et al.* Estimation of research trawl survey catchability for biomass reconstruction of the eastern Scotian Shelf. *CSAS Res Doc* 2001;**84**:

Harley SJ, Myers RA. Hierarchical Bayesian models of length-specific catchability of research trawl surveys. *Can J Fish Aquat Sci* 2001;**58**:1569–84. https://doi.org/10.1139/f01-097

He P. Swimming speeds of marine fish in relation to fishing gears. *ICES Mar Sci Symp* 1993;**196**:183–9.

Heino M, Pauli BD, Dieckmann U. Fisheries-induced evolution. *Annu Rev Ecol Evol Syst* 2015;**46**:461–80. https://doi.org/10.1146/annurev-ecolsys-112414-054339

Hoffman MD, Gelman A. The No-U-Turn sampler: adaptively setting path lengths in Hamiltonian Monte Carlo. *ArXiv* 2011;**11**:30.

Hollowed AB, Bond NA, Wildbuer TK *et al.* A framework for modeling fish and shellfish responses to future climate change. *ICES J Mar Sci* 2009;**66**:1584–94. https://doi.org/10.1093/icesjms/fsp057

Hoydal K, Rørvik CJ, Sparre P. Estimation of effective mesh sizes and their utilization in assessment:model, gear parameters, fishing mortality, population dynamics. *Dana* 1982;**2**:69–95.

Hsieh C, Yamauchi A, Nakazawa T *et al.* Fishing effects on age and spatial structures undermine population stability of fishes. *Aquat Sci* 2010;**72**:165–78. https://doi.org/10.1007/s00027-009-0122-2

Ingólfsson ÓA, Jørgensen T. Escapement of gadoid fish beneath a commercial bottom trawl: relevance to the overall trawl selectivity. *Fish Res* 2006;**79**:303–12.

Jacobsen NS, Gilsason H, Andersen KH. The consequences of balanced harvesting of fish communities. *Proc R Soc B Biol Sci* 2013;**281**:20132701. https://doi.org/10.1098/rspb.2013.2701

Johannessen OM, Bengtsson L, Miles MW *et al.* Arctic climate change: observed and modelled temperature and sea-ice variability. *Tellus A: Dyn Meteorol Oceanogr* 2004;**56**:328–41. https://doi.org/10.3402/tellusa.v56i4.14418

Johnston IA, Dunn J. Temperature acclimation and metabolism in ectotherms with particular reference to teleost fish. *Symp Soc Exp Biol* 1987;**41**:67–93.

Jones EG, Summerbell K, O'Neill F. The influence of towing speed and fish desnity on the behaviour of haddock in a trawl cod-end. *Fish Res* 2008;**94**:166–74. https://doi.org/10.1016/j.fishres.2008.06.010

Jørgensen OA. Pelagic occurrence of Greenland halibut, *Reinhardtius hippoglossoides* (Walbaum), in west Greenland waters. *J Northwest Atl Fish Sci* 1997;**21**:39–50. https://doi.org/10.2960/J.v21.a3

Killen SS, Nati JJH, Suski CD. Vulnerability of individual fish to capture by trawling is influenced by capacity for anaerobic metabolism. *Proc Royal Soc B Biol Sci* 2015;**282**:20150603. https://doi.org/10.1098/rspb.2015.0603

King JR, Shuter BJ, Zimmerman AP. Empirical links between thermal habitat, fish growth, and climate change. *Trans Amer Fish Soc* 1999;**128**:656–65. https://doi.org/10.1577/1548-8659(1999)128⟨3c0656:ELBTHF⟩3e2.0.CO;2

Krag LA, Hermann B, Karlsen JD. Inferring fish escape behaviour in trawls based on catch comparison data: model development and evaluation based on data from Skagerrak, Denmark. *PLoS One* 2014;**9**:e88819. https://doi.org/10.1371/journal.pone.0088819

Krogh A. The quantitative relation between temperature and standard metabolism in animals. *Int Zeit Physik-Chem Biol* 1914;**1**:491–508.

Krumsick KJ, Fisher JAD. Community size spectra provide indicators of ecosystem recovery on the Newfoundland and Labrador shelf .*Mar Ecol Prog Ser* 2020;**635**:123–137. https://doi.org/10.3354/meps13212

Lacroix G, Barbut L, Volckaert FAM. Complex effect of projected sea temperature and wind change on flatfish dispersal. *Global Change Biol* 2017;**24**:85–100. https://doi.org/10.1111/gcb.13915

Larsen RB, Herrmann B, Brinkhof J *et al.* Catch efficiency of groundgears in a bottom trawl fishery: a case study of the Barents Sea haddock. *Mar Coast Fish* 2018;**10**:493–507. https://doi.org/10.1002/mcf2.10048

Law R, Grey DR. Evolution of yields from populations with age-specific cropping. *Evol Ecol* 1989;**3**:343–59. https://doi.org/10.1007/BF02285264

Law R, Plank MJ, James A *et al.* Size spectra dynamics from stochastic predation and growth of individuals. *Ecology* 2009;**90**:802–11. https://doi.org/10.1890/07-1900.1

Lefort S, Aumont O, Bopp L *et al.* Spatial and body-size dependent response of marine pelagic communities to projected global climate change. *Global Chang Bio* 2015;**21**:154–64. https://doi.org/10.1111/gcb.12679

Lett C, Ayata S-D, Huret M *et al.* Biophysical modelling to investigate the effects of climate change on marine population dispersal and connectivity. *Prog Oceanogr* 2010;**87**:106–13. https://doi.org/10.1016/j.pocean.2010.09.005

Lorenzen K. Allometry of natural mortality as a basis for assessing optimal release size in fish-stocking programmes. *Can J Fish Aquat Sci* 2000;**57**:2374–81. https://doi.org/10.1139/f00-215

Macpherson E, Gordoa A. Trends in the demersal fish community off Namibia from 1983 to 1990. *S Afr J Mar Sci* 1992;**12**:635–49. https://doi.org/10.2989/02577619209504729

Margalida A, Oro D, Cortés-Avizanda A *et al.* Misleading population estimates: biases and consistency of visual surveys and matrix modeling in the endangered bearded vulture. *PLoS One* 2011;**6**:e26784. https://doi.org/10.1371/journal.pone.0026784

Marin V, Arranz I, Grenouillet G *et al.* Fish size spectrum as a complementary biomonitoring approach of freshwater ecosystems. *Ecol Indic* 2023;**146**:109833. https://doi.org/10.1016/j.ecolind.2022.109833

Maury O, Poggiale JC. From individuals to populations to communities: a dynamic energy budget model of marine ecosystem size-spectrum including life history diversity. *J Theor Biol* 2013;**324**:52–71. https://doi.org/10.1016/j.jtbi.2013.01.018

Millar RB, Fryer RJ. Estimating the size-selection curves of towed gears, traps, nets and hooks. *Rev Fish Biol Fish* 1999;**9**:89–116. https://doi.org/10.1023/A:1008838220001

Millar RB. Estimating the size-selectivity of fishing gear by condition on the total catch. *J Amer Stat Assoc* 1992;**87**:962–8. https://doi.org/10.1080/01621459.1992.10476250

Møller PR, Renaud CB, Alfonso NR *et al. Marine Fishes of Arctic Canada*. In: Brian W. Coad, James D. Reist (eds.), Toronto: University of Toronto Press, 2018.

Mous PJ, van Densen WLT, Machiels MAM. The effect of smaller mesh sizes on catching larger fish with trawls. *Fish Res* 2002;**54**:171–9. https://doi.org/10.1016/S0165-7836(00)00304-0

NAFO. *Convention on Cooperation in the Northwest Atlantic Fisheries*. Halifax: NAFO, 2020, 47.

Ottersen G, Hjermann DØ, Stenseth NC. Changes in spawning stock structure strengthens the link between climate and recruitment in a heavily fish cod (*Gadus morhua*) stock. *Fish Oceanogr* 2006;**15**:230–43. https://doi.org/10.1111/j.1365-2419.2006.00404.x

Pauly D. On the interrelationships between natural mortality, growth parameters, and mean environmental temperature in 175 fish stocks. *ICES J Mar Sci* 1980;**39**:175–92. https://doi.org/10.1093/icesjms/39.2.175

Peng S, Zhenlin L, Liuyi H *et al.* Relationship between trawl selectivity and fish body size in a simulated population. *Chin J Oceanol Limol* 2013;**31**:327–33.

Pennington M. Estimating the relative abundance of fish from a series of trawl surveys. *Biometrics* 1985;**41**:197–202. https://doi.org/10.2307/2530654

Perry AL, Low PJ, Ellis JR *et al.* Climate change and distribution shifts in marine fishes. *Science* 2005;**308**:1912–5. https://doi.org/10.1126/science.1111322

R Core Team. 2022. *R: a language and environment for statistical computing*. Vienna: R Foundation for Statistical Computing. https://www.r-project.org/

Rice J, Gislason H. Patterns of change in the size spectra of numbers and diversity of North Sea fish assemblage, as refelected in surveys and models. *ICES J Mar Sci* 1996;**53**:1214–25. https://doi.org/10.1006/jmsc.1996.0146

Ricker WE. Production and utilization of fish populations. *Ecol Monogr* 1946;**16**:373–91. https://doi.org/10.2307/1961642

Robert M, Cortay A, Morfin M *et al.* A methodological framework for characterizing fish swimming and escapement behaviors in trawls. *PLoS One* 2020;**15**:e0243311. https://doi.org/10.1371/journal.pone.0243311

Rochet MJ, Benoît E. Fishing destabilizes the biomass flow in the marine size spectrum. *Proc R Soc B Biol Sci* 2011;**279**:284–92. https://doi.org/10.1098/rspb.2011.0893

Rosing M, Wieland K. Preliminary Results from Shrimp Trawl Calibration Experiments Off West Greenland (2004, 2005) with Notes on Encountered Experiment Design/Analyses Problems. *NAFO SCR* 2015;**5**:92

Rubner M. Concerning the influence of body size on energy metabolism. *Z Biol* 1883;**19**:536–62.

Ryer CH. A review of flatfish behavior relative to trawls. *Fish Res* 2008;**90**:138–46. https://doi.org/10.1016/j.fishres.2007.10.005

Seibel BA, Drazen JC. The rate of metabolism in marine animals: environmental constraints, ecological demands and energetic opportunities. *Phil Trans R Soc B Biol Sci* 2007;**362**:2061–78. https://doi.org/10.1098/rstb.2007.2101

Sheldon RW, Parsons TR. A continuous size spectrum for particulate matter in the sea. *J Fish Res Board Can* 1967;**24**:909–15. https://doi.org/10.1139/f67-081

Shin Y-J, Rochet MJ, Jennings S *et al.* Using size-based indicators to evaluate the ecosystem effects of fishing. *ICES J Mar Sci* 2005;**62**:384–96. https://doi.org/10.1016/j.icesjms.2005.01.004

Sissenwine MP, Bowman EW. An analysis of some factors affecting the catchability of fish by bottom trawls. *ICNAF Res Bull* 1978;**13**:81–8.

Smith J. Use of statistical models for the estimation of abundance of groundfish trawl survey data. *Can J Fish Aquat Sci* 1990;**47**:894–903. https://doi.org/10.1139/f90-103

Smith JA, Taylor MD. A peaked logistic-based selection curve. *Can J Fish Aquat Sci* 2014;**71**:351–5. https://doi.org/10.1139/cjfas-2013-0401

Somerton D. Estimating trawl catchability. *AFSC Quarterly Report April–May-June* 1996:1–3.

Stan Development Team. 2022. RStan: The R Interface to Stan. R package version 2.21.7. http://mc-stan.org/

Stepputtis D, Santos J, Hermann B *et al.* Broadening the horizon of size selectivity in trawl gears. *Fish Res* 2016;**184**:18–25. https://doi.org/10.1016/j.fishres.2015.08.030

Tam JC, Link JS, Rossberg AG *et al.* Towards ecosystem-based management: identifying operational food-web indicators for marine ecosystems. *ICES J Mar Sci* 2017;**74**:2040–52. https://doi.org/10.1093/icesjms/fsw230

Thompson PM, Harwood J. Methods for estimating the population size of common seals, *Phoca vitulina*. *J Appl Ecol* 1990;**27**:924–38. https://doi.org/10.2307/2404387

Thorson JT, Clarke ME, Stewart IJ *et al.* The implications of spatially varying catchability on bottom trawl surveys of fish abundance: a proposed solution involving underwater vehicles. *Can J Fish Aquat Sci* 2012;**70**:294–306.

Thorson JT, Prager MH. Better catch curves: incorporating age-specific natural mortality and logistic selectivity. *Trans Amer Fish*

Soc 2011;**140**:356–66. https://doi.org/10.1080/00028487.2011.557016

Treble MA, Nogueira A. Assessment of the Greenland Halibut stock component in NAFO subarea 0 + 1 (offshore). *NAFO SCR Doc* 2020;**38**:1–31.

Turner LJ, Mackay WC. Use of visual census for estimating population size in northern pike (*Esox lucius*). *Can J Fish Aquat Sci* 1985;**42**:1835–40. https://doi.org/10.1139/f85-231

Vehtari A, Gelman A, Gabry J. Practical Bayesian model evaluation using leave-one-out cross-validation and WAIC. *Stat Comput* 2017;**27**:1413–32. https://doi.org/10.1007/s11222-016-9696-4

Vehtari A, Gelman A, Simpson D *et al*. Rank-normalization, folding, and localization: an improved R-hat for assessing convergence of MCMC (with discussion). *Bayesian Data Anal* 2021;**16**:667–718.

Videler, JJ, Wardle CS. Fish swimming stride by stride: speed limits and endurance .*Rev Fish Biol Fish* 1991;**1**:23–40.

Weinberg KL, Yeung C, Somerton DA *et al*. Is the survey selectivity curve for Pacific cod (*Gadus macrocephalus*) dome shaped? Direct evidence from trawl studies. *Fish Bull* 2016;**114**:360–70. https://doi.org/10.7755/FB.114.3.8

West G, Brown J, Enquist B. A general model for the origin of allometric scaling laws in biology. *Science* 1997;**276**:122–6. https://doi.org/10.1126/science.276.5309.122

West G, Brown JH, Enquist BJ. A general model for ontogenetic growth. *Nature* 2001;**413**:628–31. https://doi.org/10.1038/35098076

Wheeland LJ, Morgan MJ. Age-specific shifts in Greenland halibut (*Reinhardtius hippoglossoides*). *ICES J Mar Sci* 2020;**77**:230–40.

White GC, Bennetts RE. Analysis of frequency count data using the negative binomial distribution. *Ecology* 1996;**77**:2549–57. https://doi.org/10.2307/2265753

Winger PD, Eayrs S, Glass CW. Fish behavior near bottom trawls. In: P He (ed.), *Behavior of Marine Fishes: Capture Processes and Conservation Challenges*. Ames, IA: Wiley-Blackwell, 2010, 67–103.

Winger PD, He P, Walsh SJ. Swimming endurance of American plaice (*Hippoglossoides platessoides*) and its role in fish capture. *ICES J Mar Sci* 1999;**56**:252–65. https://doi.org/10.1006/jmsc.1999.0441

Woodworth-Jefcoats PA, Polovina JJ, Dune JP *et al*. Ecosystem size structure response to 21st century climate projection: large fish abundance decreases in the central North Pacific and increases in the California Current. *Global Change Biol* 2013;**19**:724–33. https://doi.org/10.1111/gcb.12076

Xiaojun X, Ruyung S. The bioenergetics of the souther catfish (*Silurus meridionalis* Chen). I. Resting metabolic rate as a function of body weight and temperature. *Physio Zool* 1990;**63**:1181–95. https://doi.org/10.1086/physzool.63.6.30152639

Xu C, Gertner GZ. Uncertainty and sensitivity analysis for models with correlated parameters. *Reliab Eng Syst Saf* 2008;**93**:1563–73. https://doi.org/10.1016/j.ress.2007.06.003

Xu N, Delius GW, Lai Z *et al*. Spatial drivers of instability in marine size spectrum ecosystems. *J Theor Bio* 2021;**517**:110631. https://doi.org/10.1016/j.jtbi.2021.110631

Yvon-Durocher G, Montoya JM, Trimmer M *et al*. Woodward alters the size spectrum and shifts the distribution of biomass in freshwater ecosystems. *Glob Change Biol* 2011;**17**:1681–94. https://doi.org/10.1111/j.1365-2486.2010.02321.x

Zagarese HE, Williamson CE. The implications of solar UV radiation exposure for fish and fisheries. *Fish Fish* 2001;**2**:250–60. https://doi.org/10.1046/j.1467-2960.2001.00048.x

Zhang C, Chen Y, Ren Y. Assessing uncertainty of a multispecies size-spectrum model resulting from process and observation errors. *ICES J Mar Sci* 2015;**71**:2223–33. https://doi.org/10.1093/icesjms/fsv086

Handling Editor: Stan Kotwicki